
Ellipsoidal Trust Region Methods for Neural Nets

Leonard Adolphs*, Jonas Kohler*, Aurelien Lucchi

Department of Computer Science

ETH Zurich

{ladolphs, jonas.kohler, aurelien.lucchi}@inf.ethz.ch

Abstract

We investigate the use of ellipsoidal trust region constraints for second-order optimization of neural networks. This approach can be seen as a higher-order counterpart of adaptive gradient methods, which we here show to be interpretable as first-order trust region methods with ellipsoidal constraints. In particular, we show that the preconditioning matrix used in RMSProp and Adam satisfies the necessary conditions for convergence of (first- and) second-order trust region methods and report that this ellipsoidal constraint constantly outperforms its spherical counterpart in practice.

1 Introduction

We consider finite-sum optimization problems of the form

$$\mathbf{w}^* = \arg \min_{\mathbf{w} \in \mathbb{R}^d} \left[\mathcal{L}(\mathbf{w}) := \sum_{i=1}^n \ell(f(\mathbf{w}, \mathbf{x}_i), \mathbf{y}_i) \right], \quad (1)$$

which typically arise in neural network training, e.g. for empirical risk minimization over a set of data points $(\mathbf{x}_i, \mathbf{y}_i) \in \mathbb{R}^{in} \times \mathbb{R}^{out}$, $i = 1, \dots, n$. Here, $\ell : \mathbb{R}^{out} \times \mathbb{R}^{out} \rightarrow \mathbb{R}^+$ is a convex loss and $f : \mathbb{R}^{in} \times \mathbb{R}^d \rightarrow \mathbb{R}^{out}$ represents the neural network mapping parameterized by $\mathbf{w} \in \mathbb{R}^d$, which is non-convex due to its multiplicative nature and potentially non-linear activation functions. We assume that \mathcal{L} is twice differentiable, i.e. $\mathcal{L} \in C^2(\mathbb{R}^d, \mathbb{R})$.

In the era of big data and deep neural networks, stochastic gradient descent (SGD) is one of the most widely used training algorithms [3]. However, gradient descent is known to be inadequate to optimize functions that are not well-conditioned [28, 33] and thus adaptive first-order methods that employ dynamic, coordinate-wise learning rates based on past gradients – including Adagrad [13], RMSprop [34] and Adam [19] – have become a popular alternative to SGD.

From a theoretical perspective, Newton methods provide stronger convergence guarantees by appropriately transforming the gradient in ill-conditioned regions according to second-order derivatives. It is precisely this Hessian information that allows *regularized* Newton methods to enjoy superlinear local convergence as well as to escape saddle points [9], which can slow gradient methods down significantly [12] and are believed to be prevalent in high dimensional problems [11]. Among the class of regularized Newton methods, trust region [9] and cubic regularization algorithms [6] are the most principled approaches, as they yield the strongest convergence guarantees. Recently, stochastic extensions have emerged [37, 38, 20, 16], which suggest their applicability for deep learning.

We here propose a further simple modification to make TR methods even more suitable for neural network training. Particularly, we build up on the following alternative interpretation of adaptive gradient methods (Section 3):

While gradient descent can be interpreted as a spherically constrained first-order TR method, preconditioned gradient methods can be seen as first-order TR methods with ellipsoidal constraint sets. We

* Equal contribution.

leverage this analogy and investigate the use of the Adagrad and RMSProp preconditioning matrices as *ellipsoidal* trust region shapes within *second-order* TR methods. While the theory for ellipsoidal TR methods is well-studied (e.g. [9, 39]), no ellipsoid fits all objective functions and our contribution thus lies in the identification of adequate matrix-induced constraints for the specific task of deep learning that yield provable convergence guarantees. Furthermore, we empirically show that the ellipsoidal constraints we propose prove to be a very effective modification of the trust region method in the sense that they constantly outperform the spherical TR method, both in terms of number of backpropagations and asymptotic loss value on a variety of tasks and datasets.

2 Related work

The most principled class of regularized Newton methods are trust region (TR) and adaptive cubic regularization algorithms (ARC) [9, 6], which repeatedly optimize a local Taylor model of the objective while making sure that the step does not travel too far such that the model stays accurate. While the former finds first-order stationary points within $\mathcal{O}(\epsilon_g^{-2})$, ARC only takes at most $\mathcal{O}(\epsilon_g^{-3/2})$. However, simple modifications to the TR framework allow these methods to obtain the same accelerated rate [10]. Both methods take at most $\mathcal{O}(\epsilon_H^{-3})$ iterations to find an ϵ_H approximate second-order stationary point [5]. These rates are optimal for second-order Lipschitz continuous functions [4, 5] and they can be retained even when only sub-sampled gradient and Hessian information is used [20, 38, 37, 2, 22, 7]. Furthermore, the involved Hessian information can be computed solely based on Hessian-vector products, which are implementable efficiently for neural networks [32]. This makes these methods particularly attractive for deep learning, but the empirical evidence of their applicability is so far very limited. We are only aware of the works of [22] and [36], which report promising first results but these are by no means fully encompassing. While the former does not benchmark any first-order method at all, the latter uses large batch sizes and neither trains convolutional networks nor benchmarks any adaptive gradient method. Finally, an interesting line of research proposes to replace the use of the Hessian with the Generalized Gauss Newton matrix [25, 24, 26, 23].

3 An alternative view on adaptive gradient methods

Adaptive gradient methods update iterates as $\mathbf{w}_{t+1} = \mathbf{w}_t - \eta_t \mathbf{A}_t^{-1/2} \mathbf{g}_t$, where \mathbf{g}_t is a stochastic estimate of $\nabla \mathcal{L}(\mathbf{w}_t)$ and \mathbf{A}_t is a positive definite symmetric pre-conditioning matrix. In RMSProp and Adam, $\mathbf{A}_{rms,t}$ is the un-centered second moment matrix of exponentially weighted past gradients which we compute as follows

$$\mathbf{A}_{rms,t} := ((1 - \beta) \mathbf{G}_t \text{diag}(\beta^t, \dots, \beta^0) \mathbf{G}_t^\top) + \epsilon \mathbf{I}, \quad (2)$$

where $\beta \in (0, 1)$. In order to save computational efforts, the diagonal version $\text{diag}(\mathbf{A}_{rms})$ is more commonly applied in practice, which in turn gives rise to coordinate-wise adaptive stepsizes that are enlarged (reduced) in coordinates that have seen past gradient components with a smaller (larger) magnitude. In that way, the optimization methods can account for gradients of potentially different scales arising from e.g., different layers of the networks. Based on this observation, one can take a principled view of these methods. Namely, their update steps arise from minimizing a first-order Taylor model of the function \mathcal{L} within an *ellipsoidal* search space around the current iterate \mathbf{w}_t , where the diameter of the ellipsoid along a certain coordinate is proportional to the associated stepsize. Fig. 2 in the Appendix illustrates this effect.

Theorem 1 (Preconditioned gradient methods as TR). *A preconditioned gradient step*

$$\mathbf{w}_{t+1} - \mathbf{w}_t = \mathbf{s}_t := -\eta_t \mathbf{A}_t^{-1} \mathbf{g}_t \quad (3)$$

with stepsize $\eta_t > 0$, symmetric positive definite preconditioner $\mathbf{A}_t \in \mathbb{R}^{d \times d}$ and $\mathbf{g}_t \neq 0$ minimizes a first order model around $\mathbf{w}_t \in \mathbb{R}^d$ in an ellipsoid given by \mathbf{A}_t in the sense that

$$\mathbf{s}_t := \arg \min_{\mathbf{s} \in \mathbb{R}^d} [m_t^1(\mathbf{s}) = \mathcal{L}(\mathbf{w}_t) + \mathbf{s}^\top \mathbf{g}_t], \quad \text{s.t.} \quad \|\mathbf{s}\|_{\mathbf{A}_t} \leq \eta_t \|\mathbf{g}_t\|_{\mathbf{A}_t^{-1}}. \quad (4)$$

4 Second-order Trust Region Methods

Cubic regularization [29, 6] and trust region methods belong to the family of globalized Newton methods. Both frameworks compute their parameter updates by optimizing regularized (former) or constrained (latter) second-order Taylor models of the objective \mathcal{L} around the current iterate \mathbf{w}_t .

$$\min_{\mathbf{s} \in \mathbb{R}^d} \left[m_t(\mathbf{s}) := \mathcal{L}(\mathbf{w}_t) + \mathbf{g}_t^\top \mathbf{s} + \frac{1}{2} \mathbf{s}^\top \mathbf{B}_t \mathbf{s} \right], \quad \text{s.t. } \|\mathbf{s}\|_{\mathbf{A}_t} \leq \Delta_t \quad (5)$$

where $\Delta_t > 0$ and \mathbf{g}_t and \mathbf{B}_t are either $\nabla \mathcal{L}(\mathbf{w}_t)$ and $\nabla^2 \mathcal{L}(\mathbf{w}_t)$ or suitable approximations. The matrix \mathbf{A}_t induces the shape of the constraint set. So far, the common choice for neural networks is $\mathbf{A}_t := \mathbf{I}$, $\forall t$ which gives rise to spherical trust regions [36, 22]. One crucial condition for convergence is that the applied norms are not degenerate during the minimization process in the sense that the ellipsoids do not flatten out completely along any given direction.

Definition 1 (Uniformly equivalent norms). The norms $\|\mathbf{w}\|_{\mathbf{A}_t} := (\mathbf{w}^\top \mathbf{A}_t \mathbf{w})^{1/2}$ induced by symmetric positive definite matrices \mathbf{A}_t are called uniformly equivalent, if there exists a constant $\mu \geq 1$ such that $1/\mu \|\mathbf{w}\|_{\mathbf{A}_t} \leq \|\mathbf{w}\|_2 \leq \mu \|\mathbf{w}\|_{\mathbf{A}_t}$, $\forall \mathbf{w} \in \mathbb{R}^d, \forall t = 1, 2, \dots$.

Proposition 1 (Uniform equivalence). *Suppose $\|\mathbf{g}_t\|^2 \leq L_H^2$ for all $\mathbf{w}_t \in \mathbb{R}^d, t = 1, 2, \dots$. Then there always exists $\epsilon > 0$ such that the proposed preconditioning matrices $\mathbf{A}_{rms,t}$ (Eq. (2)) are uniformly equivalent, i.e. Def. 1 holds. The same holds for the diagonal variant.*

Consequently, the ellipsoids \mathbf{A}_{rms} can directly be applied to any convergent TR framework without losing convergence guarantees ([9], Theorem 6.6.8).

Why ellipsoids? There are many sources for ill-conditioning in neural networks such as un-centered and correlated inputs [21], saturated hidden units and different weight scales in different layers of the network [35]. While the quadratic term in the model (5) does account for such ill-conditioning to some extent, the spherical constraint is completely blind towards the loss surface but it is in general advisable to instead measure distances in norms that reflect the underlying geometry (Chapter 7.7 in [9]). The ellipsoids we propose are such that they allow for longer steps along coordinates that have seen small gradient components in the past and vice versa. Thereby the TR shape is adaptively adjusted to fit the current region of the non-convex loss landscape.

Algorithmic framework We here opt for a fully stochastic TR framework [8] in order to circumvent memory issues and reduce computational complexity. Given that the involved function and derivative estimates are sufficiently accurate with fixed probability, such a framework has been shown to retain the convergence rate of deterministic TR methods to stationary points in expectation [2]. For finite-sum objectives such as Eq. (1) the required level of accuracy can be obtained by simple mini-batching. In that case, Algorithm 1 with \mathbf{A}_{rms} ellipsoids converges with the classical $O(\epsilon^{-2}, \epsilon^{-3})$ thanks to Proposition 2 and Theorem 6.6.8 in [9].

Algorithm 1 Stochastic Ellipsoidal Trust Region Method

- 1: **Input:** $\mathbf{w}_0 \in \mathbb{R}^d, \gamma_1, \gamma_2 > 1, 1 > \eta_2 > \eta_1 > 0, \Delta_0 > 0, T \geq 1, |\mathcal{S}_0|, \mu \geq 1, \epsilon > 0$
- 2: **for** $t = 0, 1, \dots$, **until convergence do**
- 3: Sample $\mathcal{L}_t, \mathbf{g}_t$ and \mathbf{B}_t with batch sizes $|\mathcal{S}_{\mathcal{L},t}|, |\mathcal{S}_{\mathbf{g},t}|, |\mathcal{S}_{\mathbf{B},t}|$
- 4: Compute preconditioner \mathbf{A}_t s.t. Def. 1 holds
- 5: Obtain \mathbf{s}_t by solving $m_t(\mathbf{s}_t)$ (Eq. (5))
- 6: Compute actual over predicted decrease on batch

$$\rho_{\mathcal{S},t} = \frac{\mathcal{L}_{\mathcal{S}}(\mathbf{w}_t) - \mathcal{L}_{\mathcal{S}}(\mathbf{w}_t + \mathbf{s}_t)}{m_t(\mathbf{0}) - m_t(\mathbf{s}_t)} \quad (6)$$

- 7: Set

$$\Delta_{t+1} = \begin{cases} \gamma_1 \Delta_t & \text{if } \rho_{\mathcal{S},t} > \eta_2 \text{ (very successful)} \\ \Delta_t & \text{if } \eta_2 \geq \rho_{\mathcal{S},t} \geq \eta_1 \text{ (successful)}, \mathbf{w}_{t+1} = \begin{cases} \mathbf{w}_t + \mathbf{s}_t & \text{if } \rho_{\mathcal{S},t} \geq \eta_1 \\ \mathbf{w}_t & \text{otherwise} \end{cases} \\ \Delta_t / \gamma_2 & \text{if } \rho_{\mathcal{S},t} < \eta_1 \text{ (unsuccessful)} \end{cases}$$

- 8: **end for**
-

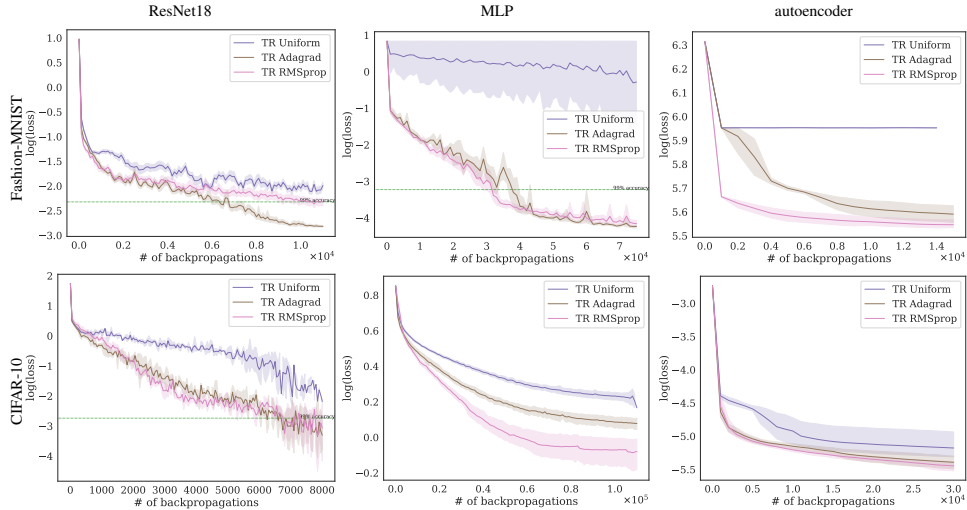


Figure 1: Log loss over number of backprops. Average and 95% CI of 10 independent runs. Green dotted line indicates 99% accuracy.

The main difference between Algorithm 1 and most existing approaches in [20, 37, 38, 7] lies in the computation of ρ , which is traditionally computed as full function- over stochastic model decrease. Computing ρ solely based on sub-sampled quantities has the nice side-effect of disentangling two potential sources of error: an overoptimistic trust region radius and insufficiently small batch sizes.

5 Experiments

To validate our claim that ellipsoidal TR methods yield improved performance over spherical ones, we run a set of experiments on two image datasets and three types of network architectures. The TR methods use 512 samples for both the gradient and Hessian computation, except for the ResNet18 architecture on CIFAR-10 where we use 128 sample, due to memory constraints. The ellipsoids are based on *diagonal* pre-conditioners and we employ the Steihaug-Toint Conjugate Gradient method ([9], Alg. 7.5.1) as subproblem solver. More details can be found in Appendix C.

As can be seen in Figure 1, the ellipsoidal TR methods consistently outperform the spherical counterpart in the sense that they reach full training accuracy substantially faster on all problems. Furthermore, their limit points are in all cases lower than those of the uniform TR method and especially on the autoencoders this makes an actual difference in the image reconstruction quality (see Figure 5). We thus draw the clear conclusion that the ellipsoidal trust region constraints we propose are to be preferred over their spherical counterpart when training neural networks.

6 Conclusion

We investigated the use of ellipsoidal trust region constraints for neural networks. We have shown that the RMSProp matrix satisfies the necessary conditions for convergence, and our experimental results demonstrate that ellipsoidal TR methods outperform their spherical counterparts significantly. We thus consider the development of further ellipsoids that can potentially adapt even better to the loss landscape such as, e.g. (block-) diagonal Hessian approximations (see [1]) or approximations of higher order derivatives as an interesting direction of future research.

Interestingly, an empirical benchmark with gradient methods (Appendix A) indicates that the value of Hessian information for neural network optimization is limited for mainly three reasons: 1) second-order methods rarely yield better limit points, which suggests that saddles and spurious local minima are not a major obstacle; 2) gradient methods can run on smaller batch sizes which is beneficial in terms of epoch and when memory is limited; 3) finally, the per-iteration time complexity is noticeably lower for first-order methods. In summary, these observations suggest that advances in hardware and distributed second-order algorithms (e.g., [30, 14]) will be needed to speed up computations before Newton-type methods can replace (stochastic) gradient methods in deep learning.

References

- [1] Costas Bekas, Effrosyni Kokiopoulou, and Yousef Saad. An estimator for the diagonal of a matrix. *Applied numerical mathematics*, 57(11-12):1214–1229, 2007.
- [2] Jose Blanchet, Coralia Cartis, Matt Menickelly, and Katya Scheinberg. Convergence rate analysis of a stochastic trust region method for nonconvex optimization. *arXiv preprint arXiv:1609.07428*, 2016.
- [3] Leon Bottou. Large-scale machine learning with stochastic gradient descent. In *Proceedings of COMPSTAT'2010*, pages 177–186. Springer, 2010.
- [4] Yair Carmon, John C Duchi, Oliver Hinder, and Aaron Sidford. Lower bounds for finding stationary points i. *arXiv preprint arXiv:1710.11606*, 2017.
- [5] Coralia Cartis, Nicholas IM Gould, and Ph L Toint. Complexity bounds for second-order optimality in unconstrained optimization. *Journal of Complexity*, 28(1):93–108, 2012.
- [6] Coralia Cartis, Nicholas IM Gould, and Philippe L Toint. Adaptive cubic regularisation methods for unconstrained optimization. part i: motivation, convergence and numerical results. *Mathematical Programming*, 127(2):245–295, 2011.
- [7] Coralia Cartis and Katya Scheinberg. Global convergence rate analysis of unconstrained optimization methods based on probabilistic models. *Mathematical Programming*, pages 1–39, 2017.
- [8] Ruobing Chen, Matt Menickelly, and Katya Scheinberg. Stochastic optimization using a trust-region method and random models. *Mathematical Programming*, 169(2):447–487, 2018.
- [9] Andrew R Conn, Nicholas IM Gould, and Philippe L Toint. *Trust region methods*. SIAM, 2000.
- [10] Frank E Curtis, Daniel P Robinson, and Mohammadreza Samadi. A trust region algorithm with a worst-case iteration complexity of $\mathcal{O}(\epsilon^{3-2})$ for nonconvex optimization. *Mathematical Programming*, 162(1-2):1–32, 2017.
- [11] Yann N Dauphin, Razvan Pascanu, Caglar Gulcehre, Kyunghyun Cho, Surya Ganguli, and Yoshua Bengio. Identifying and attacking the saddle point problem in high-dimensional non-convex optimization. In *Advances in neural information processing systems*, pages 2933–2941, 2014.
- [12] Simon S Du, Chi Jin, Jason D Lee, Michael I Jordan, Aarti Singh, and Barnabas Poczos. Gradient descent can take exponential time to escape saddle points. In *Advances in Neural Information Processing Systems*, pages 1067–1077, 2017.
- [13] John Duchi, Elad Hazan, and Yoram Singer. Adaptive subgradient methods for online learning and stochastic optimization. *Journal of Machine Learning Research*, 12(Jul):2121–2159, 2011.
- [14] Celestine Düner, Aurelien Lucchi, Matilde Gargiani, An Bian, Thomas Hofmann, and Martin Jaggi. A distributed second-order algorithm you can trust. *arXiv preprint arXiv:1806.07569*, 2018.
- [15] Gabriel Goh. Why momentum really works. *Distill*, 2017.
- [16] Serge Gratton, Clément W Royer, Luís N Vicente, and Zaikun Zhang. Complexity and global rates of trust-region methods based on probabilistic models. *IMA Journal of Numerical Analysis*, 2017.
- [17] Geoffrey E Hinton and Ruslan R Salakhutdinov. Reducing the dimensionality of data with neural networks. *science*, 313(5786):504–507, 2006.
- [18] Stanislaw Jastrzebski, Zachary Kenton, Devansh Arpit, Nicolas Ballas, Asja Fischer, Yoshua Bengio, and Amos Storkey. Three factors influencing minima in sgd. *arXiv preprint arXiv:1711.04623*, 2017.
- [19] Diederik P Kingma and Jimmy Ba. Adam: A method for stochastic optimization. *arXiv preprint arXiv:1412.6980*, 2014.
- [20] Jonas Moritz Kohler and Aurelien Lucchi. Sub-sampled cubic regularization for non-convex optimization. In *International Conference on Machine Learning*, 2017.
- [21] Yann A LeCun, Léon Bottou, Genevieve B Orr, and Klaus-Robert Müller. Efficient backprop. In *Neural networks: Tricks of the trade*, pages 9–48. Springer, 2012.

- [22] Liu Liu, Xuanqing Liu, Cho-Jui Hsieh, and Dacheng Tao. Stochastic second-order methods for non-convex optimization with inexact hessian and gradient. *arXiv preprint arXiv:1809.09853*, 2018.
- [23] James Martens. Deep learning via hessian-free optimization. In *ICML*, volume 27, pages 735–742, 2010.
- [24] James Martens. New insights and perspectives on the natural gradient method. *arXiv preprint arXiv:1412.1193*, 2014.
- [25] James Martens and Roger Grosse. Optimizing neural networks with kronecker-factored approximate curvature. In *International conference on machine learning*, pages 2408–2417, 2015.
- [26] James Martens and Ilya Sutskever. Training deep and recurrent networks with hessian-free optimization. In *Neural networks: Tricks of the trade*, pages 479–535. Springer, 2012.
- [27] Dominic Masters and Carlo Luschi. Revisiting small batch training for deep neural networks. *arXiv preprint arXiv:1804.07612*, 2018.
- [28] Yurii Nesterov. *Introductory lectures on convex optimization: A basic course*, volume 87. Springer Science & Business Media, 2013.
- [29] Yurii Nesterov and Boris T Polyak. Cubic regularization of newton method and its global performance. *Mathematical Programming*, 108(1):177–205, 2006.
- [30] Kazuki Osawa, Yohei Tsuji, Yuichiro Ueno, Akira Naruse, Rio Yokota, and Satoshi Matsuoka. Second-order optimization method for large mini-batch: Training resnet-50 on imagenet in 35 epochs. *arXiv preprint arXiv:1811.12019*, 2018.
- [31] Adam Paszke, Sam Gross, Soumith Chintala, Gregory Chanan, Edward Yang, Zachary DeVito, Zeming Lin, Alban Desmaison, Luca Antiga, and Adam Lerer. Automatic differentiation in pytorch. 2017.
- [32] Barak A Pearlmutter. Fast exact multiplication by the hessian. *Neural computation*, 6(1):147–160, 1994.
- [33] Shai Shalev-Shwartz, Ohad Shamir, and Shaked Shammah. Failures of gradient-based deep learning. *arXiv preprint arXiv:1703.07950*, 2017.
- [34] Tijmen Tieleman and Geoffrey Hinton. Lecture 6.5-rmsprop: Divide the gradient by a running average of its recent magnitude. *COURSERA: Neural networks for machine learning*, 4(2):26–31, 2012.
- [35] Patrick Van Der Smagt and Gerd Hirzinger. Solving the ill-conditioning in neural network learning. In *Neural networks: tricks of the trade*, pages 193–206. Springer, 1998.
- [36] Peng Xu, Farbod Roosta-Khorasan, and Michael W Mahoney. Second-order optimization for non-convex machine learning: An empirical study. *arXiv preprint arXiv:1708.07827*, 2017.
- [37] Peng Xu, Farbod Roosta-Khorasani, and Michael W Mahoney. Newton-type methods for non-convex optimization under inexact hessian information. *arXiv preprint arXiv:1708.07164*, 2017.
- [38] Zhewei Yao, Peng Xu, Farbod Roosta-Khorasani, and Michael W Mahoney. Inexact non-convex newton-type methods. *arXiv preprint arXiv:1802.06925*, 2018.
- [39] Ya-xiang Yuan. Recent advances in trust region algorithms. *Mathematical Programming*, 151(1):249–281, 2015.
- [40] Matthew D Zeiler. Adadelata: an adaptive learning rate method. *arXiv preprint arXiv:1212.5701*, 2012.

Appendix A: Ommited figures

A Illustration of Theorem 1

The following figure depicts the iterates of GD and Adagrad along with the implicit trust regions within which the local models were optimized at each step.¹ Since the models are linear, the constrained minimizer is always found on the boundary of the current trust region.

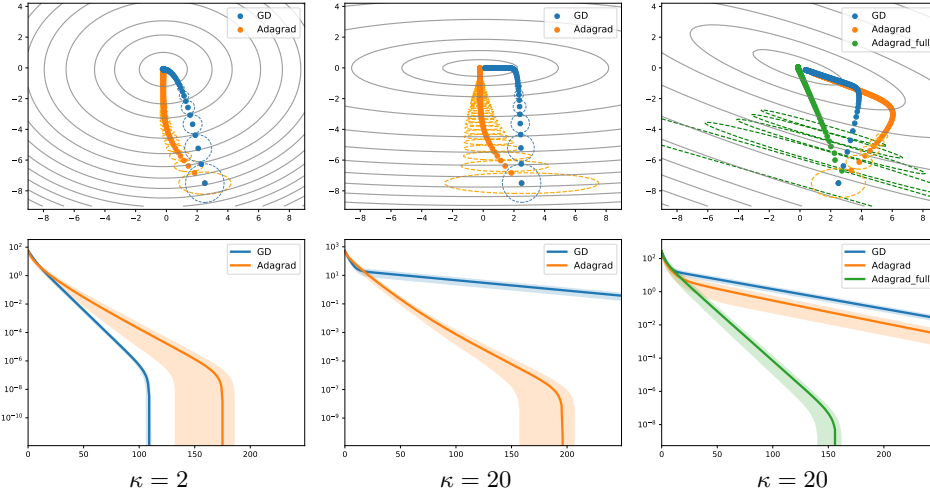


Figure 2: Top: Iterates and implicit trust regions of GD and Adagrad on three quadratic objectives with different condition number κ . Bottom: Average log suboptimality over iterations as well as 90% confidence intervals of 30 runs with random initialization

As illustrated by the dashed trust region lines, Adagrad’s search space is damped along the direction of high curvature (vertical axis) and elongated along the low curvature direction (horizontal axis). This preconditioning allows the method to move further horizontally early on and thus enter the valley with a smaller distance to the optimizer \mathbf{w}^* along the low curvature direction which effectively circumvents the fact that GD struggles to progress towards the minimizer of quadratics along low-curvature directions (see e.g. [15]). Interestingly, as can be seen on the far right, full matrix preconditioning (*Adagrad full*) is very effective when the coordinates are interdependent (i.e. the Hessian is not diagonally dominant).

B SGD benchmark

Benchmark with SGD In order to put the results of Section 5 into context, we benchmark several first-order methods on the same problem set, for which we fix the sample size for all gradient methods to 32 (as advocated e.g. in [27]) but grid search the stepsize since it is the ratio of these two quantities that effectively determines the level of stochasticity [18]. As the TR methods have a larger batch size², we report results both in terms of number of backpropagations and epochs for a fair comparison.

A close look at Figure 3 and 4 indicates that the ellipsoidal TR methods are slightly superior in terms of backprops but only just so manage to keep pace with first-order methods in terms of epochs. Furthermore, the limit points of both first- and second-order methods yield the same order of loss in most experiments. When taking gradient norms into account (plot omitted) we indeed find no spurious local minima and only the autoencoder architecture gives rise to saddle points. Thus, the net value of adding Hessian information to the update steps appears rather marginal when it comes to

¹For illustrative purposes we only plot every other trust region.

²In our experiments, we observed weaker performance when running TR with small mini-batches. We hypothesize that second-order methods extract more information of each batch per step and are thus more likely to "overfit" small batches.

optimizing neural networks. This is particularly the case if computational time is limited, since each second-order step takes considerably more time than a gradient update.

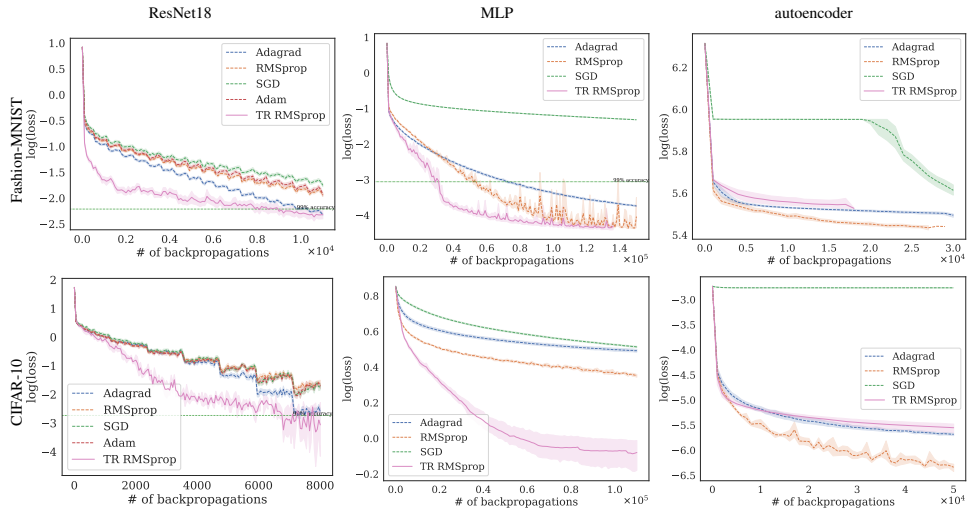


Figure 3: Log loss over **backprops**. Same setting as Figure 1.

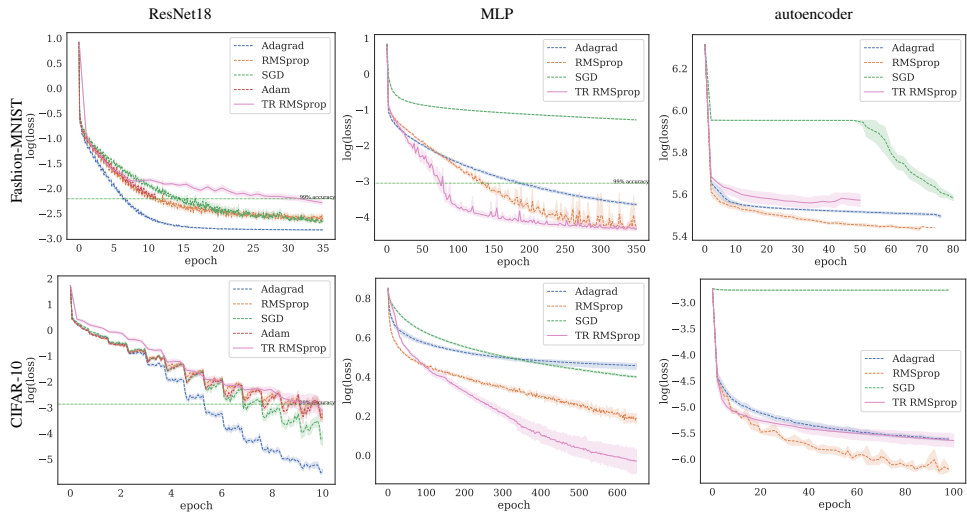


Figure 4: Log loss over **epochs**. Same setting as Figure 1.

Appendix B: Proofs

Notation Scalars are denoted by regular lower case letters, vectors by bold lower case letters and matrices as well as tensors by bold upper case letters. By $\|\cdot\|$ we denote an arbitrary norm. For a symmetric positive definite matrix \mathbf{A} we introduce the compact notation $\|\mathbf{w}\|_{\mathbf{A}} = (\mathbf{w}^T \mathbf{A} \mathbf{w})^{1/2}$, where $\mathbf{w} \in \mathbb{R}^d$.

C Equivalence of Preconditioned Gradient Descent and First Order Trust Region Methods

Theorem 2 (Theorem 1 restated). *A preconditioned gradient step*

$$\mathbf{w}_{t+1} - \mathbf{w}_t = \mathbf{s}_t := -\eta_t \mathbf{A}_t^{-1} \mathbf{g}_t \quad (7)$$

with stepsize $\eta_t > 0$, symmetric positive definite preconditioner $\mathbf{A}_t \in \mathbb{R}^{d \times d}$ and $\mathbf{g}_t \neq 0$ minimizes a first order local model around $\mathbf{w}_t \in \mathbb{R}$ in an ellipsoid given by \mathbf{A}_t in the sense that

$$\begin{aligned} \mathbf{s}_t &:= \arg \min_{\mathbf{s} \in \mathbb{R}^d} [m_t^1(\mathbf{s}) = \mathcal{L}(\mathbf{w}_t) + \mathbf{s}^\top \mathbf{g}_t], \\ \text{s.t. } &\|\mathbf{s}\|_{\mathbf{A}} \leq \eta_t \|\mathbf{g}_t\|_{\mathbf{A}^{-1}}. \end{aligned} \quad (8)$$

Proof. We start the proof by noting that the optimization problem (8) is convex. For $\eta_t > 0$ the constraint satisfies the Slater condition since 0 is a strictly feasible point. As a result, any KKT point is a feasible minimizer and vice versa.

Let $L(\mathbf{s}, \lambda)$ denote the Lagrange dual of (4), i.e. $L(\mathbf{s}, \lambda) := \mathcal{L}(\mathbf{w}_t) + \mathbf{s}^\top \mathbf{g}_t + \lambda (\|\mathbf{s}\|_{\mathbf{A}} - \eta_t \|\mathbf{g}_t\|_{\mathbf{A}^{-1}})$.

Any point \mathbf{s} is a KKT point if and only if the following system of equations is satisfied

$$\nabla_{\mathbf{s}} L(\mathbf{s}, \lambda) = \mathbf{g}_t + \frac{\lambda}{\|\mathbf{s}\|_{\mathbf{A}}} \mathbf{A} \mathbf{s} = 0 \quad (9)$$

$$\lambda (\|\mathbf{s}\|_{\mathbf{A}} - \eta_t \|\mathbf{g}_t\|_{\mathbf{A}^{-1}}) = 0. \quad (10)$$

$$\|\mathbf{s}\|_{\mathbf{A}} - \eta_t \|\mathbf{g}_t\|_{\mathbf{A}^{-1}} \leq 0 \quad (11)$$

$$\lambda \geq 0. \quad (12)$$

For \mathbf{s}_t as given in Eq. (3) we have that $\|\mathbf{s}_t\|_{\mathbf{A}} = \sqrt{\eta_t^2 \mathbf{g}_t^\top (\mathbf{A}^{-1})^\top \mathbf{A} \mathbf{A}^{-1} \mathbf{g}_t} = \eta_t \sqrt{\mathbf{g}_t^\top \mathbf{A}^{-1} \mathbf{g}_t} = \eta_t \|\mathbf{g}_t\|_{\mathbf{A}^{-1}}$ and thus (10) and (11) hold with equality such that any $\lambda \geq 0$ is feasible. Furthermore,

$$\nabla_{\mathbf{s}} L(\mathbf{s}_t, \lambda) = \nabla f(\mathbf{w}_t) + \frac{\lambda}{\|\mathbf{s}_t\|_{\mathbf{A}}} \mathbf{A} \mathbf{s}_t \stackrel{(3)}{=} \mathbf{g}_t - \eta_t \frac{\lambda}{\eta_t \|\mathbf{g}_t\|_{\mathbf{A}^{-1}}} \mathbf{A} \mathbf{A}_t^{-1} \mathbf{g}_t = \mathbf{g}_t - \frac{\lambda}{\|\mathbf{g}_t\|_{\mathbf{A}^{-1}}} \mathbf{g}_t \quad (13)$$

is zero for $\lambda = \|\mathbf{g}_t\|_{\mathbf{A}^{-1}} \geq 0$. As a result, \mathbf{s}_t is a KKT point of the convex Problem (4) which proves the assertion. \square

D Convergence of ellipsoidal TR methods

Spherical constrained TR methods Under standard smoothness assumptions, spherical TR algorithms achieve ϵ_g criticality after $O(\epsilon_g^{-2})$ iterations and additionally ϵ_H almost positive curvature in $O(\epsilon_H^{-3})$ iterations (see Theorem 4.3 in [5]). Interestingly, these rates can be improved to match the (optimal) $\mathcal{O}(\epsilon^{-3/2})$ first-order worst case complexity of Cubic Regularization by applying small modifications to the TR framework [10]. For both, cubic regularization and trust region methods, many stochastic extensions have emerged in literature that alleviate the need to compute exact derivative information without losing the above mentioned convergence guarantees with high probability [20, 36, 37, 2, 16, 16]). For the deep learning setting, the analysis of [2] is most relevant since it also allows the algorithm to run solely based on sub-sampled function evaluations.

Ellipsoidal constrained TR methods In order to prove such results for ellipsoidal Trust Region methods one must ensure that the applied norms are coherent during the complete minimization process in the sense that the ellipsoids do not flatten out (or blow up) completely along any given direction. This intuition is formalized in Assumption 1 which we restate here for the sake of clarity.

Definition 2 (Definition 1 restated). There exists a constant $\mu \geq 1$ such that

$$\frac{1}{\mu} \|\mathbf{w}\|_{\mathbf{A}_t} \leq \|\mathbf{w}\|_2 \leq \mu \|\mathbf{w}\|_{\mathbf{A}_t}, \quad \forall t = 1, 2, \dots, \forall \mathbf{w} \in \mathbb{R}^d. \quad (14)$$

Having uniformly equivalent norms is necessary and sufficient to prove that ellipsoidal TR methods enjoy the same convergence rate as classical ball constrained Trust Region algorithms.

Towards this end, [9] identify the following sufficient condition on the basis of which we will prove that our proposed ellipsoid \mathbf{A}_{rms} is indeed uniformly equivalent under some mild assumptions.

Lemma 1 (Theorem 6.7.1 in [9]). *Suppose that there exists a constant $\zeta \geq 1$ such that*

$$\frac{1}{\zeta} \leq \sigma_{\min}(\mathbf{A}_t) \leq \sigma_{\max}(\mathbf{A}_t) \leq \zeta \quad \forall t = 1, 2, \dots, \quad (15)$$

then Definition 1 holds.

Proposition 2 (Uniform equivalence). *Suppose $\|\mathbf{g}_t\|^2 \leq L_H^2$ for all $\mathbf{w}_t \in \mathbb{R}^d$, $t = 1, 2, \dots$. Then there always exists $\epsilon > 0$ such that the proposed preconditioning matrices $\mathbf{A}_{rms,t}$ (Eq. (2)) are uniformly equivalent, i.e. Def. 1 holds. The same holds for the diagonal variant.*

Proof. The basic building block of our ellipsoid matrix consists of the current and past stochastic gradients $\mathbf{G}_t := [\mathbf{g}_1, \mathbf{g}_2, \dots, \mathbf{g}_t]$. We consider \mathbf{A}_{rms} which is built up as follows³

$$\mathbf{A}_{rms,t} := \left((1 - \beta) \mathbf{G} \underbrace{\text{diag}(\beta^t, \beta^{t-1}, \dots, \beta^0)}_{:=\mathbf{D}} \mathbf{G}^\top \right) + \epsilon \mathbf{I}. \quad (16)$$

From the construction of $\mathbf{A}_{rms,t}$ it directly follows that for any unit length vector $\mathbf{u} \in \mathbb{R}^d \setminus \{0\}$, $\|\mathbf{u}\|_2 = 1$ we have

$$\begin{aligned} \mathbf{u}^\top ((1 - \beta) \mathbf{G} \mathbf{D} \mathbf{G}^\top + \epsilon \mathbf{I}) \mathbf{u} &= (1 - \beta) \mathbf{u}^\top \mathbf{G} \mathbf{D}^{1/2} (\mathbf{D}^{1/2})^\top \mathbf{G}^\top \mathbf{u} + \epsilon \|\mathbf{u}\|_2^2 \\ &= (1 - \beta) \left((\mathbf{D}^{1/2})^\top \mathbf{G}^\top \mathbf{u} \right)^\top \left((\mathbf{D}^{1/2})^\top \mathbf{G}^\top \mathbf{u} \right) + \epsilon \|\mathbf{u}\|_2^2 \geq \epsilon > 0, \end{aligned} \quad (17)$$

which proves the lower bound for $\zeta = 1/\epsilon$. Now, let us consider the upper end of the spectrum of $\mathbf{A}_{rms,t}$. First, recall the geometric series expansion $\sum_{i=0}^t \beta^{t-i} = \sum_{i=0}^t \beta^i = \frac{1 - \beta^{t+1}}{1 - \beta}$ and the fact that $\mathbf{G} \mathbf{G}^\top$ is a sum of exponentially weighted rank-one positive semi-definite matrices of the form $\mathbf{g}_i \mathbf{g}_i^\top$. Thus

$$\lambda_{\max}(\mathbf{g}_i \mathbf{g}_i^\top) = \text{Tr}(\mathbf{g}_i \mathbf{g}_i^\top) = \|\nabla \mathbf{g}_i\|^2 \leq L_H^2,$$

where the latter inequality holds per assumption for any sample size $|S|$. Combining these facts we get that

$$\begin{aligned} \mathbf{u}^\top ((1 - \beta) \mathbf{G} \mathbf{D} \mathbf{G}^\top + \epsilon \mathbf{I}) \mathbf{u} &= (1 - \beta) \mathbf{u}^\top \mathbf{G} \mathbf{D} \mathbf{G}^\top \mathbf{u} + \epsilon \|\mathbf{u}\|_2^2 \\ &= (1 - \beta) \sum_{i=0}^t \beta^{t-i} \mathbf{u}^\top \mathbf{g}_i \mathbf{g}_i^\top \mathbf{u} + \epsilon \|\mathbf{u}\|_2^2 \leq (1 - \beta) \sum_{i=0}^t \beta^{t-i} L_H^2 \|\mathbf{u}\|_2^2 + \epsilon \|\mathbf{u}\|_2^2 \\ &= (1 - \beta^{t+1}) L_H^2 + \epsilon. \end{aligned} \quad (18)$$

As a result we have that

$$\epsilon \leq \lambda_{\min}(\mathbf{A}_{rms,t}) \leq \lambda_{\max}(\mathbf{A}_{rms,t}) \leq (1 - \beta^{t+1}) L_H^2 + \epsilon \quad (19)$$

Finally, to achieve uniform equivalence we need the r.h.s. of (19) to be bounded by $1/\epsilon$. This gives rise to a quadratic equation in ϵ , namely $\epsilon^2 + (1 - \beta^{t+1}) L_H^2 \epsilon - 1 \leq 0$ which holds for any t and any $\beta \in (0, 1)$ as long as

$$0 \leq \epsilon \leq \frac{1}{2} (\sqrt{L_H^4 + 4} - L_H^2). \quad (20)$$

³This is a generalization of the diagonal variant proposed by [34], which precondition the gradient step by an elementwise division with the square-root of the following estimate $g_t = (1 - \beta)g_{t-1} + \beta \nabla \mathcal{L}(\mathbf{w}_t)^2$.

Such an ϵ always exists but one needs to choose smaller and smaller values as the upper bound on the gradient norm grows. For example, the usual value $\epsilon = 10^{-8}$ is valid for all $L_H^2 < 9.9 \cdot 10^7$. All of the above arguments naturally extend to the diagonal preconditioner $\text{diag}(\mathbf{A}_{rms})$.

□

Interestingly, this result cannot be established for the Adagrad inspired ellipsoid \mathbf{A}_{ada} , which reflects the commonly noticed effect that the stepsizes of first-order Adagrad shrink over time as squared gradients are continuously added to the preconditioning matrix. It is mainly this effect that eventually inspired the development of Rmsprop [34], Adadelta [40] and simliar approaches.

Appendix C: Experiment details

A Default parameters, architectures and datasets

| | $ \mathcal{S}_0 $ | Δ_0 | Δ_{\max} | η_1 | η_2 | γ_1 | γ_2 | κ_K (krylov tol.) |
|--------|-------------------|------------|-----------------|-----------|----------|------------|------------|--------------------------|
| TR_uni | 512 | 10^{-4} | 10 | 10^{-4} | 0.95 | 1.1 | 1.5 | 0.1 |
| TR_ada | 512 | 10^{-4} | 10 | 10^{-4} | 0.95 | 1.1 | 1.5 | 0.1 |
| TR_rms | 512 | 10^{-4} | 10 | 10^{-4} | 0.95 | 1.1 | 1.75 | 0.1 |

Table 1: Default parameters

Parameters Table 1 reports the default parameters we consider. Only for the larger ResNet18 on CIFAR-10, we adapted the batch size to 128 due to memory constraints. For the sake of comparability, $\text{TR}_{\text{uniform}}$ and $\text{TR}_{\text{adagrad}}$ are always run with the same parameters and hence the only difference is in the trust region shape. TR_{rms} shares most of these parameters but we sometimes start with a smaller TR radius and have a higher decrease (γ_2) since we observed that RMSprop usually also runs on much slower learning rates than SGD and Adagrad.

Datasets We use two real-world datasets for image classification, namely CIFAR-10 and Fashion-MNIST. While Fashion-MNIST consists of greyscale 28×28 images, CIFAR-10 are colored images of size 32×32 . We emply a fixed training-test split consisting of 50,000 (60,000 for Fashion-MNIST) training and 10,000 test images, respectively.

Network architectures The MLP architectures are simple. For MNIST and Fashion-MNIST we use a $784 - 128 - 10$ network with tanh activations and a cross entropy loss. The networks has $101'770$ parameters. For the CIFAR-10 MLP we use a $3072 - 128 - 128 - 10$ architecture also with tanh activations and cross entropy loss. This network has $410'880$ parameters.

The MNIST and Fashion-MNIST autoencoders have the same architecture as the ones used in [17, 36, 23, 25]. The encoder structure is $784 - 1000 - 500 - 250 - 30$ and the decoder is mirrored. Sigmoid activations are used in all but the central layer. The reconstructed images are fed pixelwise into a binary cross entropy loss. The network has a total of $2'833'000$ parameters. The CIFAR-10 autoencoder is taken from the implementation of <https://github.com/jellycsc/PyTorch-CIFAR-10-autoencoder>.

In all of our experiments each method was run on one Tesla P100 GPU using the PyTorch [31] library.

B Reconstructed Images from Autoencoders

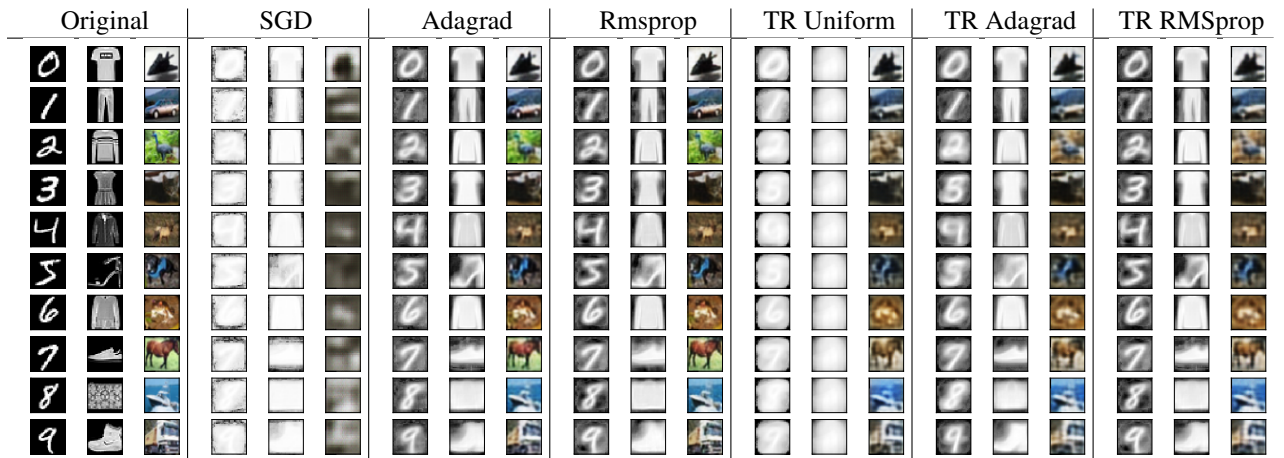


Figure 5: Original and reconstructed MNIST digits (left), Fashion-MNIST items (middle), and CIFAR-10 classes (right) for different optimization methods after convergence. Compare Figure 1 & 3 for corresponding loss.